nature climate change

LETTERS

PUBLISHED ONLINE: 10 NOVEMBER 2014 | DOI: 10.1038/NCLIMATE2436

Microbe-driven turnover offsets mineral-mediated storage of soil carbon under elevated CO_2

Benjamin N. Sulman[1,2,3]*, Richard P. Phillips[3], A. Christopher Oishi[4], Elena Shevliakova[1,5] and Stephen W. Pacala[5]

The sensitivity of soil organic carbon (SOC) to changing environmental conditions represents a critical uncertainty in coupled carbon cycle–climate models[1]. Much of this uncertainty arises from our limited understanding of the extent to which root–microbe interactions induce SOC losses (through accelerated decomposition or 'priming'[2]) or indirectly promote SOC gains (via 'protection' through interactions with mineral particles[3,4]). We developed a new SOC model to examine priming and protection responses to rising atmospheric CO_2. The model captured disparate SOC responses at two temperate free-air CO_2 enrichment (FACE) experiments. We show that stabilization of 'new' carbon in protected SOC pools may equal or exceed microbial priming of 'old' SOC in ecosystems with readily decomposable litter and high clay content (for example, Oak Ridge[5]). In contrast, carbon losses induced through priming dominate the net SOC response in ecosystems with more resistant litters and lower clay content (for example, Duke[6]). The SOC model was fully integrated into a global terrestrial carbon cycle model to run global simulations of elevated CO_2 effects. Although protected carbon provides an important constraint on priming effects, priming nonetheless reduced SOC storage in the majority of terrestrial areas, partially counterbalancing SOC gains from enhanced ecosystem productivity.

Soils contain more carbon (C) than plant biomass and the atmosphere combined[7]. Although a large body of literature has explored the effects of elevated CO_2 on plant growth[8], there is considerable uncertainty as to how such changes will affect SOC stocks[5,9]. A large fraction of this uncertainty is due to the complexity of soil processes and structure: an enormous variety of chemical compounds and a diverse community of bacteria and fungi in the soil respond in complex ways to changes in temperature, moisture and inputs of fresh plant C (refs 2,10). Furthermore, recent advances in isotopic, genomic and spectroscopic tools have revealed that a suite of physical, chemical and biological factors control not only SOC decomposition, but also SOC formation and stabilization[4,11]. Current global-scale land surface models represent SOC decay as a first-order process that depends only on abiotic factors such as temperature and moisture[1], with limited representations of root and microbial influences on SOC. Whereas microbial models have been applied at global scales[12], rhizosphere processes and microbial influences on SOC stabilization and mineralization have not previously been integrated into global land surface models. Hence, the development of global-scale SOC models that represent essential processes and interactions while remaining tractable for parameterization in Earth system models (ESMs) remains a major challenge.

There is now substantial evidence from both empirical and modelling studies that inputs of simple, readily assimilated C compounds such as glucose and amino acids (hereafter referred to as 'simple C') can accelerate the decomposition of complex organic compounds[2]. Such 'priming effects' are likely to have important consequences for global SOC stocks. Rising atmospheric CO_2 concentrations generally increase the inputs of simple C to soils through greater leaf and root production[13] and enhanced root exudation[14]. Such increases have been identified as responsible for accelerated losses of SOC in multiple CO_2-enrichment experiments[6,9,15,16], as well as in a broad synthesis of ecosystem responses to elevated CO_2 (ref. 17). The importance of priming is further supported by modelling efforts, as ecosystem models based on first-order decomposition have been unable to explain observed changes in C and N cycling under elevated CO_2 (refs 18,19), and land surface models that include coarse representations of priming have produced more accurate maps of global SOC stocks[20].

Although priming effects are critically important and globally significant, an important constraint on their impact is that plant-derived inputs can also lead to the formation of SOC that is protected from microbial degradation. There is now increasing evidence that a significant proportion of stable SOC is derived from simple C rather than chemically resistant compounds[3], and that the long-term preservation of SOC depends more on its accessibility to microbial decomposers than on its chemical complexity[4,11]. Such 'protection' of SOC results from physical occlusion in microaggregates or chemical sorption in organo-mineral complexes. Notably, protected SOC may also have lower temperature sensitivity than chemically resistant SOC, meaning that its response to future climate change could be different even if its contemporary turnover rate is the same[21].

To investigate the global consequences of SOC priming and protection, we developed a new SOC model, Carbon, Organisms, Rhizosphere, and Protection in the Soil Environment (CORPSE), that represents protected and unprotected SOC pools, and uses a dynamic microbial biomass pool to control SOC transformation and decomposition (Fig. 1). Both protected and unprotected SOC pools contain a combination of compounds with different decomposition rates and parameters. This approach is more flexible than previous formulations that represented only bulk SOC and dissolved organic C, and did not include a separate protected C pool[12]. Furthermore, CORPSE is novel in that it links microbial turnover to protected

[1]Princeton Environmental Institute, Princeton University, Princeton, New Jersey 08544, USA. [2]School of Public and Environmental Affairs, Indiana University, Bloomington, Indiana 47405, USA. [3]Department of Biology, Indiana University, Bloomington, Indiana 47405, USA. [4]USDA Forest Service, Southern Research Station, Coweeta Hydrologic Laboratory, Otto, North Carolina 28763, USA. [5]Department of Ecology and Evolutionary Biology, Princeton University, Princeton, New Jersey 08544, USA. *e-mail: bsulman@indiana.edu

© 2014 Macmillan Publishers Limited. All rights reserved.

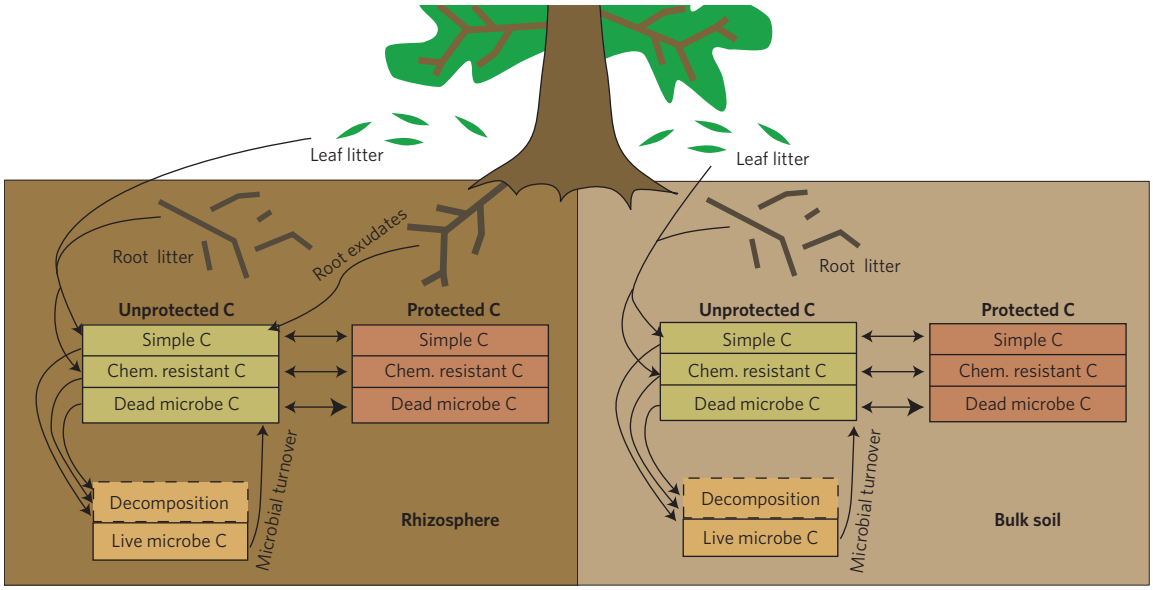

Figure 1 | Diagram of model structure. Soil carbon is divided into three chemical classes, which can be protected or unprotected. Decomposition is mediated by microbial biomass, which takes up a portion of decomposed carbon and loses carbon to CO_2 and the dead microbial C pool over time. Soil is separated into the rhizosphere, which receives root exudate inputs, and bulk soil, which does not.

C formation via a microbial necromass C pool with a rapid stabilization rate. Moreover, CORPSE has separate compartments for rhizosphere and bulk soil processes so that consequences of changes in rhizosphere volume can be quantified. The model simulates priming effects through enhanced microbial growth in response to simple C inputs. Simple C inputs also increase the rate of protected carbon formation via increased microbial biomass and turnover, following ref. 3. Because of the nonlinear response of SOC turnover to simple C inputs, the partitioning of SOC between rhizosphere (which receives root exudates) and bulk soil (which does not) has a strong influence on the overall SOC turnover rate, and expansion of the rhizosphere can greatly increase the magnitude of priming effects.

We calibrated the model using data from a previous laboratory simple C addition experiment (Supplementary Fig. 3), and applied it to the Duke and Oak Ridge National Laboratory (ORNL) decade-long free-air CO_2 enrichment (FACE) experiments. For the Duke FACE experiment, priming effects resulting from increased exudation and rhizosphere expansion largely offset the effect of enhanced leaf and root litter inputs under elevated CO_2, resulting in only a slight net increase in SOC (Fig. 2a)—well within the margin of error of previous studies[6,22]. In ORNL simulations, priming effects were much weaker whereas the protected C response was significantly stronger, resulting in greater net C accumulation (Fig. 2b). The enhanced protection of SOC at ORNL compared to Duke was primarily driven by the higher clay content of ORNL soils. Protection rate in the model is determined by clay content, although other factors such as mineralogy modify this relationship in actual soils[4]. Furthermore, ORNL leaf litter was composed of fast-turnover broadleaf species whereas Duke litter was dominated by slow-turnover needleleaf species (Supplementary Fig. 4). In general, model simulations indicated that greater litter decomposability is associated with weaker priming effects (Supplementary Fig. 8). This is due to a combination of two factors. First, rapid litter turnover leads to smaller chemically resistant SOC pools, which limits the substrate available for priming. Second, fast-decomposing litter increases the simple C available to microbes, thereby decreasing the importance of root exudation in driving microbial activity. Although the magnitude of simulated SOC responses to elevated

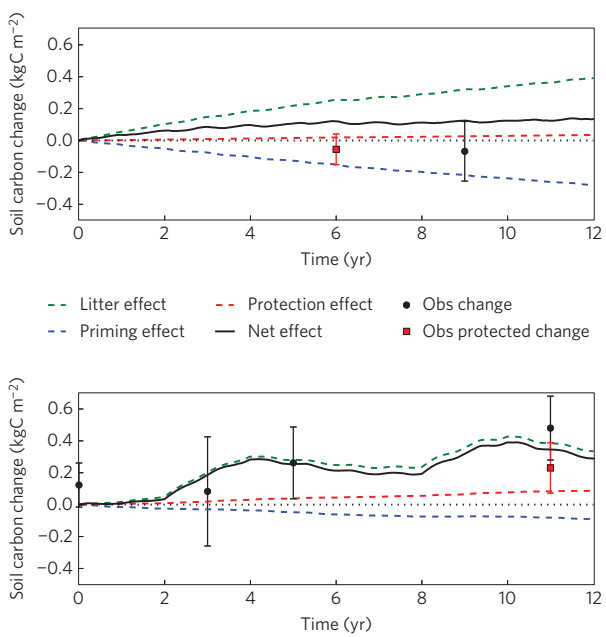

Figure 2 | Observed and modelled responses of soil carbon to elevated CO_2. Lines show modelled litter effects, priming effects, changes in protected carbon and the overall net change at Duke and ORNL FACE sites. Symbols with error bars show measured values and reported measurement standard error. **a**, Duke FACE. **b**, ORNL FACE.

CO_2 at ORNL matched observations, simulations underestimated the equilibrium protected C and total SOC pools (Supplementary Fig. 6), implying that the dependence of protected C formation on clay content is stronger than the relationship included in the model. Our model thus predicts that the net response of SOC to elevated CO_2 depends on interactions between priming effects, litter decomposability, and protected carbon formation. In ecosystems with chemically resistant litter, strong priming effects cancel most of the SOC accumulation attributable to increased productivity,

© 2014 Macmillan Publishers Limited. All rights reserved.

whereas in ecosystems with rapidly decomposing litter, priming effects are weaker and elevated CO_2 causes net increases in SOC. Soil mineralogy further impacts this balance: in soils with higher clay content, protected C formation will play a stronger role in the net SOC response, leading to more net C accumulation.

These simulated contrasts between sites matched observations: whereas the Duke FACE experiment had no detectable SOC response to elevated CO_2 (refs 6,22), observed SOC stocks in elevated CO_2 plots at the ORNL site increased substantially relative to control plots[5]. In an intercomparison, ecosystem models lacking priming effects were unable to capture this contrast in SOC responses[18]. A large fraction of observed SOC accumulation at ORNL occurred in microaggregates[5], which was also consistent with our simulations, which showed a significant increase in protected carbon at the site (Fig. 2b). Furthermore, observed N uptake at the Duke FACE experiment significantly increased under elevated CO_2, which is consistent with enhanced priming effects[6]. At the ORNL FACE experiment, the increase in N uptake was much smaller, eventually leading to progressive N limitation[18,23].

We embedded the new SOC model (CORPSE) within the Geophysical Fluid Dynamics Laboratory (GFDL) global land model LM3 (refs 24,25) to demonstrate interactions between rhizosphere priming and SOC protection at global scales. We conducted simulations over a thirty-year period and compared how priming induced by elevated exudation and expanded rhizosphere volume (owing to elevated atmospheric CO_2 comparable to that of the FACE experiments) impacted global SOC. Rhizosphere priming decreased total SOC over the majority of terrestrial areas, with the strongest effects occurring in temperate North America, Western Europe, Southeast Asia and Southern Africa (Fig. 3a). Despite enhanced rhizosphere activity, other regions experienced SOC gains, as exudation stimulated protected C formation. These areas included boreal North America, Siberia and tropical South America. Whereas in high latitude regions this effect was mainly the result of decomposition being limited by cold temperatures rather than substrate chemistry, priming effects were limited in tropical South America because warm temperatures and abundant moisture supported rapid decomposition, depleting available substrates and the potential for additional increases in decomposition. Furthermore, this region was characterized by soils with a high clay content that enhanced the formation of protected carbon (Supplementary Fig. 9).

Increases in net primary production (NPP) due to CO_2 fertilization led to additional SOC accumulation owing to increased C inputs (Fig. 3b). This contradicts results from a previous microbial modelling study suggesting that SOC stocks were independent of NPP (ref. 12). Although losses due to priming effects were generally not enough to outweigh these gains, SOC accumulation due to CO_2 fertilization was reduced by 30–50% in regions with strong priming effects (Fig. 3c). Although our global simulations were designed as a test of important processes rather than a quantitatively accurate depiction of the earth system, our results suggest that enhanced root activity driven by rising atmospheric CO_2 could cause a loss on the order of 25 Pg of chemically resistant soil carbon, partially mitigated by the accumulation of up to 6 Pg of additional protected carbon (Supplementary Table 1).

The importance of rhizosphere expansion in simulating strong priming effects (Supplementary Fig. 7) highlights the need to consider this aspect of soil biogeochemical heterogeneity. At present, the fraction of soil volume considered part of the rhizosphere is subject to great uncertainty, and is rarely explicitly considered in either models or field measurements of priming effects. Further research is needed to constrain rhizosphere volume, its response to ecological changes such as enhanced plant growth and root exudation, and its role in ecosystem-level priming effects.

As well as for SOC, our results have important implications for vegetation responses to elevated CO_2: in ecosystems with

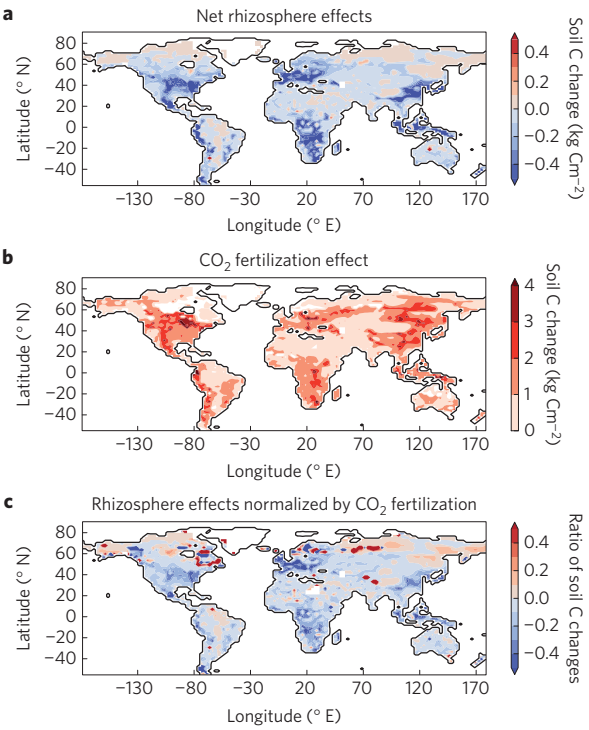

Figure 3 | Simulated priming and CO_2 fertilization effects on soil carbon at global scales. a, Net change in carbon stocks caused by increased exudation rates and rhizosphere volume. Priming effects dominated, causing net carbon loss over large regions. **b**, Increase in soil carbon stocks due to enhanced NPP under higher atmospheric CO_2. **c**, Exudation and rhizosphere expansion effects as a fraction of CO_2 fertilization effect on SOC. In some regions, priming reduced soil carbon gains by 40–50%.

decomposition-resistant litter and large chemically resistant SOC pools, priming of SOC decomposition could significantly accelerate nitrogen mineralization, supporting continued elevation of NPP. These effects could be more limited in ecosystems characterized by quickly decomposing litter. Our results highlight the importance of separating chemically resistant and physically protected carbon in both measurements and models: the two pools have contrasting responses to both climate change and litter properties, and the balance between them determines the net effect of elevated CO_2 on total SOC. The partial cancellation of priming and protection responses to root exudation implies that models that do not include both processes could overestimate either the vulnerability of SOC stocks (if they include only priming) or the potential for additional carbon storage (if they include only protection). Our results suggest that SOC responses to elevated CO_2 could be highly variable between ecosystems, depending on dominant plant species, climate and soil mineralogy. However, the net effect of enhanced root exudation is likely to be a significant reduction in global SOC stocks that counteracts the additional carbon storage expected from CO_2 fertilization.

Methods

Carbon in the CORPSE model is divided into three chemical classes representing simple and chemically resistant plant-derived compounds and microbe-derived carbon, each with a different maximum degradation rate and microbial uptake efficiency (Fig. 1). Each carbon pool can also contain multiple isotope tracers that do not affect decomposition rates but allow the model to track the fate of labelled inputs. These chemical classes can exist in both unprotected and protected forms. Protected carbon is inaccessible to microbes, and therefore cannot be decomposed until it is converted back into unprotected carbon.

Decomposition rate is determined by a temperature-dependent maximum enzymatic conversion rate, the size of the unprotected carbon pool, and the ratio

© 2014 Macmillan Publishers Limited. All rights reserved.

of microbial biomass to unprotected carbon. The dependence on microbial biomass is expressed in the form of a reverse Michaelis–Menten saturation. With this model form, the decomposition rate scales linearly with total carbon, as long as the ratio of microbial biomass to unprotected carbon remains constant.

The microbial biomass budget represents the balance between uptake of decomposed substrate carbon and the loss of biomass carbon through the combination of cell death and maintenance respiration. Microbes convert a fraction of decomposed carbon into microbial biomass, with a different microbial uptake efficiency for each class. Chemically resistant carbon has a lower uptake efficiency because its complex structure requires more energy expenditure to decompose[3]. As a result, a higher simple carbon content causes more rapid microbial growth and faster decomposition rates. Microbes lose biomass at a first-order turnover rate, which represents the combination of microbial death and maintenance respiration. Microbial turnover rate depends on the substrate carbon composition, with simple carbon inducing a faster turnover.

The protected carbon pool represents the combination of physical protection in microaggregates and organo-mineral complexes. This carbon is inaccessible to microbes and therefore not subject to decomposition until it is released to the unprotected carbon pool. Carbon moves from the unprotected to the protected pool at a class-specific rate. Carbon derived from microbial turnover has a much higher protection rate, because it is more reactive and binds easily to mineral particles[3,26]. Protected carbon moves back to the unprotected pool at a fixed, first-order rate. The equations, parameter values and additional model details are provided in the Supplementary Methods.

We calibrated the microbial and decomposition parameters using published data from an incubation experiment that used isotope-labelled glucose to measure the responses of microbial biomass and decomposition to additions of a simple substrate[27]. We ran the model at the ecosystem scale using measured temperature, moisture, litter inputs and exudation rates from the Duke and ORNL FACE experiments, and calibrated protected carbon parameters using site measurements of microaggregate and mineral-associated C. See Supplementary Methods for details.

For global simulations, we integrated CORPSE into the Geophysical Fluid Dynamics Laboratory (GFDL) global land model (LM3; refs 24,25). LM3 simulates vegetation carbon uptake and growth as well as soil physical and hydrologic processes. We calculated root exudation as a fraction of NPP, calibrated to match observed root exudation rates at the Duke FACE experiment[6]. Rhizosphere volume was calculated as a function of fine root biomass, calibrated to match the values used in the site-scale simulations. First, the model was run for 400 years by cycling pre-industrial climate simulations (years 1062–1112) from a version of the GFDL Earth system model ESM2M (ref. 28). A control simulation, a simulation with elevated root exudation and rhizosphere volume, and a simulation with elevated NPP were then continued for a further 30 years (using climate from years 1900 to 1930). Mean soil carbon values from the last five years of the simulations were compared to establish the effect of elevated root exudation. Land use was not included in the simulations. See Supplementary Methods for details. Quantitative analysis and data visualization were performed using the Matplotlib Python library.

Received 14 May 2014; accepted 25 September 2014; published online 10 November 2014

References

1. Todd-Brown, K. E. O., Hopkins, F. M., Kivlin, S. N., Talbot, J. M. & Allison, S. D. A framework for representing microbial decomposition in coupled climate models. *Biogeochemistry* **109,** 19–33 (2011).
2. Kuzyakov, Y. Priming effects: Interactions between living and dead organic matter. *Soil Biol. Biochem.* **42,** 1363–1371 (2010).
3. Cotrufo, M. F., Wallenstein, M. D., Boot, C. M., Denef, K. & Paul, E. A. The Microbial Efficiency-Matrix Stabilization (MEMS) framework integrates plant litter decomposition with soil organic matter stabilization: Do labile plant inputs form stable soil organic matter? *Glob. Change Biol.* **19,** 988–995 (2013).
4. Von Lützow, M. *et al.* Stabilization of organic matter in temperate soils: Mechanisms and their relevance under different soil conditions—a review. *Eur. J. Soil Sci.* **57,** 426–445 (2006).
5. Jastrow, J. D. *et al.* Elevated atmospheric carbon dioxide increases soil carbon. *Glob. Change Biol.* **11,** 2057–2064 (2005).
6. Drake, J. E. *et al.* Increases in the flux of carbon belowground stimulate nitrogen uptake and sustain the long-term enhancement of forest productivity under elevated CO_2. *Ecol. Lett.* **14,** 349–357 (2011).
7. Fischlin, A. *et al.* in *Climate Change 2007: Impacts, Adaptation and Vulnerability* (eds Parry, M. L., Canziani, O. F., Palutikof, J. P., van der Linden, P. J. & Hanson, C. E.) 211–272 (IPCC, Cambridge Univ. Press, 2007).
8. Denman, K. *et al.* in *Climate Change 2007: The Physical Science Basis* (eds Solomon, S. *et al.*) 499–587 (IPCC, Cambridge Univ. Press, 2007).
9. Carney, K. M., Hungate, B. A., Drake, B. G. & Megonigal, J. P. Altered soil microbial community at elevated CO_2 leads to loss of soil carbon. *Proc. Natl Acad. Sci. USA* **104,** 4990–4995 (2007).
10. Panikov, N. Understanding and prediction of soil microbial community dynamics under global change. *Appl. Soil Ecol.* **11,** 161–176 (1999).
11. Schmidt, M. W. I. *et al.* Persistence of soil organic matter as an ecosystem property. *Nature* **478,** 49–56 (2011).
12. Wieder, W. R., Bonan, G. B. & Allison, S. D. Global soil carbon projections are improved by modelling microbial processes. *Nature Clim. Change* **3,** 909–912 (2013).
13. Norby, R. J. & Zak, D. R. Ecological lessons from Free-Air CO_2 Enrichment (FACE) experiments. *Annu. Rev. Ecol. Evol. Syst.* **42,** 181–203 (2011).
14. Phillips, R. P., Finzi, A. C. & Bernhardt, E. S. Enhanced root exudation induces microbial feedbacks to N cycling in a pine forest under long-term CO_2 fumigation. *Ecol. Lett.* **14,** 187–194 (2011).
15. Talhelm, A. F., Pregitzer, K. S. & Zak, D. R. Species-specific responses to atmospheric carbon dioxide and tropospheric ozone mediate changes in soil carbon. *Ecol. Lett.* **12,** 1219–1228 (2009).
16. Hoosbeek, M. R. More new carbon in the mineral soil of a poplar plantation under Free Air Carbon Enrichment (POPFACE): Cause of increased priming effect? *Glob. Biogeochem. Cycles* **18,** GB1040 (2004).
17. Van Groenigen, K-J., Qi, X., Osenberg, C. W., Luo, Y. & Hungate, B. A. Faster decomposition under increased atmospheric CO_2 limits soil carbon storage. *Science* **344,** 508–509 (2014).
18. Zaehle, S. *et al.* Evaluation of 11 terrestrial carbon–nitrogen cycle models against observations from two temperate Free-Air CO_2 Enrichment studies. *New Phytol.* **202,** 803–822 (2014).
19. Cheng, W. *et al.* Synthesis and modeling perspectives of rhizosphere priming. *New Phytol.* **201,** 31–44 (2014).
20. Foereid, B., Ward, D. S., Mahowald, N., Paterson, E. & Lehmann, J. The sensitivity of carbon turnover in the Community Land Model to modified assumptions about soil processes. *Earth Syst. Dynam.* **5,** 211–221 (2014).
21. Davidson, E. A. & Janssens, I. A. Temperature sensitivity of soil carbon decomposition and feedbacks to climate change. *Nature* **440,** 165–173 (2006).
22. Lichter, J. *et al.* Soil carbon sequestration and turnover in a pine forest after six years of atmospheric CO_2 enrichment. *Ecology* **86,** 1835–1847 (2005).
23. Norby, R. J., Warren, J. M., Iversen, C. M., Medlyn, B. E. & McMurtrie, R. E. CO_2 enhancement of forest productivity constrained by limited nitrogen availability. *Proc. Natl Acad. Sci. USA* **107,** 19368–19373 (2010).
24. Shevliakova, E. *et al.* Carbon cycling under 300 years of land use change: Importance of the secondary vegetation sink. *Glob. Biogeochem. Cycles* **23,** GB2022 (2009).
25. Milly, P. C. D. *et al.* An enhanced model of land water and energy for global hydrologic and earth-system studies. *J. Hydrometeorol.* **15,** 1739–1761 (2014).
26. Six, J., Elliott, E. & Paustian, K. Soil macroaggregate turnover and microaggregate formation: A mechanism for C sequestration under no-tillage agriculture. *Soil Biol. Biochem.* **32,** 2099–2103 (2000).
27. Wu, J., Brookes, P. C. & Jenkinson, D. S. Formation and destruction of microbial biomass during the decomposition of glucose and ryegrass in soil. *Soil Biol. Biochem.* **25,** 1435–1441 (1993).
28. Dunne, J. P. *et al.* GFDL's ESM2 global coupled climate–carbon earth system models. Part I: Physical formulation and baseline simulation characteristics. *J. Clim.* **25,** 6646–6665 (2012).

Acknowledgements

Thanks to E. Brzostek and M. Midgley for helpful comments on the manuscript and to S. Malyshev for providing the high-frequency GFDL ESM forcing. B.N.S., E.S. and S.W.P. acknowledge support in parts from the NOAA (US Department of Commerce) grant NA08OAR4320752, the USDA grant 2011-67003-30373 and the Carbon Mitigation Initiative at Princeton University, sponsored by BP. The statements, findings and conclusions are those of the authors and do not necessarily reflect the views of the NOAA, the US Department of Commerce, the US Department of Agriculture, or BP.

Author contributions

B.N.S. developed the model, designed and conducted experiments, analysed the data, and wrote the paper. E.S. and S.W.P. contributed to model development and experimental design and helped write the paper. R.P.P. and A.C.O. contributed data and expertise for set-up and interpretation of site-level simulations, and helped write the paper.

Additional information

Supplementary information is available in the online version of the paper. Reprints and permissions information is available online at www.nature.com/reprints. Correspondence and requests for materials should be addressed to B.N.S.

Competing financial interests

The authors declare no competing financial interests.

© 2014 Macmillan Publishers Limited. All rights reserved.